Transport and magnetic properties of Mo2.5Ru0.5Sb7–xTex

Christophe Candolfi, Bertrand Lenoir, Anne Dauscher, Emmanuel Guilmeau, Jiří Hejtmánek

Transport and magnetic properties of $Mo_{2.5}Ru_{0.5}Sb_{7-x}Te_x$

Cite as: J. Appl. Phys. **107**, 093709 (2010); https://doi.org/10.1063/1.3388056
Submitted: 19 February 2010 • Accepted: 17 March 2010 • Published Online: 06 May 2010

C. Candolfi, B. Lenoir, A. Dauscher, et al.

Transport and magnetic properties of $Mo_{2.5}Ru_{0.5}Sb_{7-x}Te_x$

C. Candolfi,[1,a)] B. Lenoir,[1] A. Dauscher,[1] E. Guilmeau,[2] and J. Hejtmánek[3]
[1]*Institut Jean Lamour, UMR CNRS, Nancy Université, UPVM 7198, Ecole Nationale Supérieure des Mines de Nancy, Parc de Saurupt, 54042 Nancy cedex, France*
[2]*CRISMAT-ENSICAEN, CNRS, UMR 6508, 6 Bd Maréchal Juin, 14050 Caen Cedex, France*
[3]*Institute of Physics, Academy of Sciences of the Czech Republic, Cukrovarnicka 10, CZ-162 53 Praha 6, Czech Republic*

(Received 19 February 2010; accepted 17 March 2010; published online 6 May 2010)

Transport properties including electrical resistivity, thermopower, and thermal conductivity of polycrystalline $Mo_{2.5}Ru_{0.5}Sb_{7-x}Te_x$ compounds for $0 \leq x \leq 1$ have been investigated in the 2–1000 K temperature range. Additional information on the concentrations and the scattering mechanisms of the charge carriers as well as on the magnetic properties has been obtained through Hall effect and magnetic susceptibility measurements performed in the 5–300 K temperature range. The enhancement in the Te content results in a decrease in the carrier concentration which is at the origin of the simultaneous increase in the electrical resistivity and thermopower. A single parabolic band model with acoustic phonon scattering enables to explain the compositional and temperature dependence of the thermopower while such a simple model fails to adequately describe the electronic thermal conductivity. This characteristic together with the unusual dependence of the thermal conductivity upon alloying might be a direct consequence of strong phonons-dimers interactions displayed by Mo_3Sb_7. Magnetic susceptibility data demonstrate that the antiferromagnetically-coupled dimers tend to disappear as x is enhanced, lending further support to a crucial role played by these interactions to understand the thermal transport in these materials. Low thermal conductivity coupled with high thermopower values result in a high dimensionless figure of merit $ZT \sim 0.70$ at 1000 K in $Mo_{2.5}Ru_{0.5}Sb_{6.5}Te_{0.5}$ positioning this material as an interesting candidate for power generation applications. © *2010 American Institute of Physics*.
[doi:10.1063/1.3388056]

I. INTRODUCTION

Zintl phases are currently drawing great attention for their potential as thermoelectric materials.[1–6] These phases meet the requirements to achieve a high dimensionless figure of merit ZT which stands for the key factor that indicates whether or not a material is suitable for thermoelectric applications. This factor is defined as $ZT = \alpha^2 T/\rho\lambda = PT/\lambda$ where α is the Seebeck coefficient or thermopower, ρ the electrical resistivity, λ the total thermal conductivity, $P = \alpha^2/\rho$ the power factor, and T the absolute temperature.[7] Most of the Zintl phases display a complex unit cell that helps, in general, to limit the phonon mean free path, i.e., to lower the thermal conductivity. The richness of the chemical compositions and possible substitutions which can be envisaged then offers the opportunity to finely tune the electrical properties to enhance the power factor.

Several new families of Zintl phases have been discovered in the last ten years to exhibit high ZT values at high temperature positioning these materials as prospective candidates for power generation applications. Some of them, such as $Yb_{14}MnSb_{11}$ and its related compounds or $EuZn_2Sb_2$, even surpass the ZT values of the best state-of-the-art thermoelectric materials operating in the 900–1200 K temperature range in radioisotope thermoelectric generators, namely Si–Ge alloys.[8–11]

Recently, another compound whose bondings can be rationalized within the Zintl concept and crystallizing in the bcc Ir_3Ge_7 structure type (space group $Im3m$), namely Mo_3Sb_7, has been considered as a possible candidate and subsequently, its thermoelectric potential has been investigated.[1,12] Besides intriguing features such as BCS-like superconductivity (Bardeen-Cooper-Schrieffer) and a spin gap formation in its magnetic excitation spectrum at $T^* = 53$ K, this exotic metal was found to display an outstanding ZT value of ~0.20 at 1000 K.[12–23] However, such value is too low to compete with state-of-the-art thermoelectric materials, requiring further enhancement in its thermoelectric properties. Electronic band structure calculations demonstrated that providing two additional electrons per formula unit drives the system into a semiconducting state.[24–27] Experimentally, previous investigations have shown that the position of the Fermi level can be shifted up via partial substitutions of antimony by tellurium or molybdenum by ruthenium.[26–30] Even though a lower than required solubility limit (~1.6 for Te and ~0.8 for Ru) of the two aforementioned elements prevents a metal-insulator transition to occur in real compounds, both substitutions markedly affect all the relevant properties involved in thermoelectricity leading to higher ZT values near 1000 K (~0.60 and 0.45

[a)]Author to whom correspondence should be addressed. Electronic addresses: christophe.candolfi@mines.inpl-nancy.fr and candolfi@cpfs.mpg.de. Present address: Max-Planck-Institut für Chemische Physik fester Stoffe, Nöthnitzer Str. 40, 01187 Dresden, Germany.

in the $Mo_3Sb_{5.4}Te_{1.6}$ and $Mo_{2.2}Ru_{0.8}Sb_7$ compounds, respectively).[29,31]

In an effort to further improve the thermoelectric properties of these compounds, double substitution on both the Mo and Sb sites by Ru and Te, respectively, may be an interesting undertaking to lower the thermal conductivity through enhanced disorder in the unit cell. This approach might also drive the system closer to the metal-insulator transition resulting in enhanced electronic properties, i.e., in higher power factors. Even though substituting on both sites allows varying simultaneously the Ru and the Te contents, we restricted our study to a fixed Ru concentration and investigated the influence of Te on the transport properties. In this context, we report on the synthesis and transport properties measurements in the 2–1000 K temperature range of polycrystalline $Mo_{2.5}Ru_{0.5}Sb_{7-x}Te_x$ compounds with $0 \leq x \leq 1$, complemented by the results obtained for Mo_3Sb_7 for comparison purposes.

II. EXPERIMENTAL DETAILS

All polycrystalline samples investigated were prepared via a powder metallurgical route decribed in detail elsewhere.[26,27] Densification of the powdered materials was realized by hot pressing using graphite dies in an argon atmosphere at 600 °C for 2 h under 51 MPa. Structural and chemical characterizations were performed by x-ray powder diffraction (XRPD) and electron probe microanalysis (EPMA). High-purity silicon was added as an internal standard to obtain accurate lattice parameters by XRPD analysis.

All measurements were performed on samples cut from the hot pressed ingots using a diamond wire saw. Electrical resistivity, thermopower, and thermal conductivity were simultaneously measured from 3.5 to 300 K using a four-point method with separated power and probe leads on bar-shaped samples of typical dimensions of $2 \times 2 \times 10$ mm^3 in an automated system cooled by a closed-cycle refrigerator. Additional information on the charge carrier concentrations were obtained via Hall effect experiments using an ac transport measurement system option (PPMS-Quantum Design) over the 2–350 K temperature range and under a magnetic field up to 7 T. Isothermal magnetization curves were measured from 5 to 300 K in applied fields of up to 7 T using a Quantum Design magnetometer (MPMS).

Four probe electrical resistivity measurements based on the Van der Pauw method were carried out in the 300–800 K temperature range. Thermopower was measured over the 300–900 K temperature range using a standard method on a commercial system (ZEM 3, Ulvac-Riko). Thermal conductivity has been evaluated from 300 to 1000 K via thermal diffusivity measurements. For all samples, the specific heat was considered to be constant throughout the high temperature range following the Dulong–Petit law. No correction for thermal expansion at high temperature was applied. Whatever the measurement is, a good agreement has been observed at room temperature between the low and high temperature sets of data. The deviation does not exceed 12%.

TABLE I. EPMA results, lattice parameter (a), and relative density (d) of the $Mo_{2.5}Ru_{0.5}Sb_{7-x}Te_x$ compounds.

Nominal Composition	*EPMA*	a (Å)	d (%)
Mo_3Sb_7	$Mo_3Sb_{6.95}$	9.568(8)	93
$Mo_{2.5}Ru_{0.5}Sb_7$	$Mo_{2.5}Ru_{0.5}Sb_7$	9.524(9)	99
$Mo_{2.5}Ru_{0.5}Sb_{6.75}Te_{0.25}$	$Mo_{2.5}Ru_{0.5}Sb_{6.75}Te_{0.25}$	9.521(9)	95
$Mo_{2.5}Ru_{0.5}Sb_{6.5}Te_{0.5}$	$Mo_{2.5}Ru_{0.5}Sb_{6.5}Te_{0.5}$	9.524(7)	91
$Mo_{2.5}Ru_{0.5}Sb_6Te$	$Mo_{2.5}Ru_{0.3}Sb_6Te$	9.542(5)	93

III. RESULTS AND DISCUSSION

A. Structural and chemical characterizations

XRPD experiments have revealed that up to $x=0.5$ the compounds are single-phase while a small amount of secondary phases could be detected in the $x=1.0$ sample ($\sim$5 vol %). EPMA further confirmed an excellent chemical homogeneity of the former compounds with a very good correlation between the nominal and the actual compositions and corroborated the presence of $RuSb_2$ as a dominating secondary phase in the latter. This study has also shown a solubility limit of Ru close to 0.30 in the $x=1.0$ sample. Table I summarizes the actual compositions, the lattice parameters as obtained from XRPD and the relative density defined as the ratio of the measured density to the theoretical density. All the given actual compositions were obtained by considering a full occupancy on the Sb site. As can be observed, the lattice parameters increase with the Te content. Noteworthy, the strong decrease of the unit cell parameter of the $Mo_{2.5}Ru_{0.5}Sb_{7-x}Te_x$ samples with respect to the parent compound is mainly due to the Ru substitution.[28,29] In this regard, as expected from the measured actual compositions, the lattice parameters of the $x=0.25$ and 0.50 samples are close to that obtained in the ternary $Mo_{3-x}Ru_xSb_7$ compounds for $x=0.50$ (see Table I).[28,29] Thus, the larger unit cell volume of the $x=1.0$ sample mainly reflects the lower Ru content and hence, is consistent with EPMA results.

B. Transport and magnetic properties

Figures 1(a) and 1(b) show the temperature dependence of the electrical resistivity and of the thermopower, respectively, for all the samples studied. None of them exhibits a semiconductinglike behavior as revealed by a positive electrical resistivity coefficient $d\rho/dT$. This first essential result can be ascribed to the lower actual Ru content exhibited by the $x=1.0$ sample that prevents two electrons per formula unit to be added. Regardless the Te content, the thermopower is positive [Fig. 1(b)] indicative of an electrical conduction dominated by holes. The magnitude of both α and ρ increases linearly with temperature and with the Te content to reach at high temperature similar values as those measured in the ternary $Mo_{3-x}Ru_xSb_7$ and $Mo_3Sb_{7-x}Te_x$ systems.[29–31] The concomitant increase in the electrical resistivity and thermopower upon alloying suggests a rigidlike behavior of the electronic band structure as already demonstrated in the above-mentioned ternary compounds by transport properties measurements together with electronic band structure

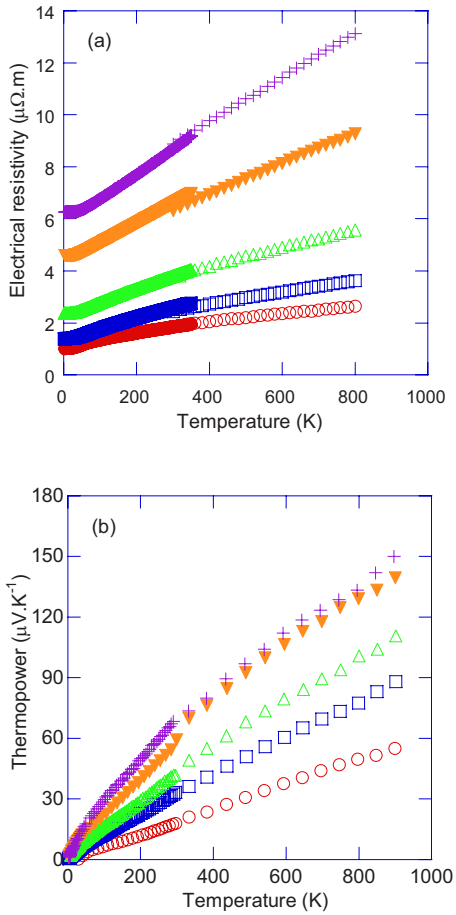

FIG. 1. (Color online) Temperature dependence of the electrical resistivity (a) and of the thermopower (b) of Mo_3Sb_7 (○) and of the $x=0.0$ (□), 0.25 (△), 0.50 (▼), and 1.0 (+) samples.

calculations.[26,27] Such behavior indicates that the electrical properties are controlled by the position of the Fermi level, i.e., by the charge carrier concentration.

Hall effect data provide compelling evidence for this picture. For all compounds, the Hall coefficient, R_H, is positive characteristic of hole conduction and, therefore, further confirms a single-carrier electrical conduction. As expected from a progressive increase in the electrical resistivity, the hole concentration p, estimated from the simple relation $p=1/R_He$ where e is the elementary charge, decreases with the Te concentration (Table II).

Using the experimental values of the electrical resistivity and Hall coefficient, the Hall mobility, $\mu_H=R_H/\rho$, can be then estimated. As shown in Fig. 2, μ_H is constant below ~20 K indicating that holes are mainly scattered by neutral

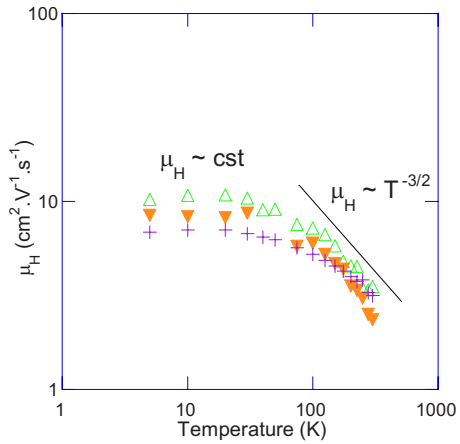

FIG. 2. (Color online) Temperature dependence of the Hall mobility, μ_H of the $x=0.25$ (△), 0.50 (▼), and 1.0 (+) compounds.

impurities. With increasing temperature, acoustic phonons then compete with neutral impurities to become the dominant scattering source above 100 K as revealed by a temperature dependence that can be modeled by a $T^{-3/2}$ law (see Fig. 2).

Additional information on the charge carriers can be obtained via the estimation of their reduced effective mass, m^*/m_0, where m_0 is the free electron mass. Within a single parabolic band model with acoustic phonon scattering as the dominating mechanism of hole diffusion near 300 K, the thermopower and the hole concentration can be expressed as[7,32]

$$\alpha = \frac{k_B}{e}\left(2\frac{F_1(\eta)}{F_2(\eta)} - \eta\right), \tag{1}$$

$$p = \frac{4}{\sqrt{\pi}}\left(\frac{2\pi m^* k_B T}{h^2}\right)^{3/2} F_{1/2}(\eta), \tag{2}$$

$$F_i(\eta) = \int_0^\infty \frac{x^i}{e^{(x-\eta)}+1}dx, \tag{3}$$

where F_i is the Fermi integral of order i, h is the Planck constant, k_B is the Boltzmann constant, and η is the reduced Fermi level. The values of the reduced effective masses and Fermi levels, calculated at 300 K, are summarized in Table III. Interestingly, the m^*/m_0 values are slightly higher than those reported in the ternary $Mo_{3-x}Ru_xSb_7$ and $Mo_3Sb_{7-x}Te_x$ compounds.[26,27] Moreover, these values remain relatively constant as a first approximation suggesting a rigid band be-

TABLE II. Hole concentration (p), Hall mobility (μ_H), Seebeck coefficient (α), electrical resistivity (ρ), and thermal conductivity (λ) measured at room temperature for the different $Mo_{3-x}Ru_xSb_{7-y}Te_y$ samples studied.

Chemical Formula	p (cm^{-3})	μ_H ($cm^2\ V^{-1}\ s^{-1}$)	α ($\mu V\ K^{-1}$)	ρ ($\mu\Omega$ m)	λ ($W\ m^{-1}\ K^{-1}$)
Mo_3Sb_7	8.5×10^{21}	4.1	18	1.8	6.2
$Mo_{2.5}Ru_{0.5}Sb_7$	2.4×10^{21}	10.0	33	2.5	5.2
$Mo_{2.5}Ru_{0.5}Sb_{6.75}Te_{0.25}$	4.6×10^{21}	3.5	44	3.8	4.9
$Mo_{2.5}Ru_{0.5}Sb_{6.5}Te_{0.5}$	4.0×10^{21}	2.3	59	6.5	4.7
$Mo_{2.5}Ru_{0.3}Sb_6Te$	2.3×10^{21}	3.2	72	8.8	4.8

TABLE III. Values of the reduced effective mass (m^*/m_0), reduced Fermi level (η), Hall factor (r_H), and Lorenz number (L) estimated assuming a single parabolic band model and acoustic phonon scattering as the dominant scattering mechanism of holes above 300 K.

Chemical Formula	m^*/m_0	η	r_H	$L_{300\ K}$ ($\times 10^{-8}$ $V^2\ K^{-2}$)	$L_{900\ K}$ ($\times 10^{-8}$ $V^2\ K^{-2}$)
Mo_3Sb_7	3.7	15.8	1.003	2.40	2.18
$Mo_{2.5}Ru_{0.5}Sb_7$	2.9	8.6	1.010	2.33	1.98
$Mo_{2.5}Ru_{0.5}Sb_{6.75}Te_{0.25}$	5.9	6.4	1.018	2.26	1.87
$Mo_{2.5}Ru_{0.5}Sb_{6.5}Te_{0.5}$	7.2	4.7	1.031	2.16	1.76
$Mo_{2.5}Ru_{0.3}Sb_6Te$	6.1	3.7	1.040	2.07	1.70

havior. To further explore this assumption, the experimental thermopower values at 300, 700, and 900 K are depicted as a function of the carrier concentration (supposed to be constant for $T>300$ K) in Fig. 3. A fit to the databased on the relations ((1))–((3)) then leads to a satisfying fit (see Fig. 3) using an average effective mass close to the room temperature value ($m^* \sim 5.2m_0$).

Note that the calculated η values obtained at 300 K offer the possibility to calculate the Hall factor, r_H, and thus, to determine whether or not the simple relation $p=r_H/R_He$ with $r_H=1$ holds in the present case. Within a single parabolic band model, r_H can be expressed as[7,32]

$$r_H = \frac{3}{4}F_{1/2}(\eta)\frac{F_{-1/2}(\eta)}{F_0^2(\eta)}. \quad (4)$$

The values of r_H, calculated at room temperature and shown in Table III, only slightly deviate from unity demonstrating that considering $r_H=1$ is reasonable to determine the hole concentration of these materials below 300 K.

Figure 4 depicts the temperature dependence of the total thermal conductivity. All the data have been corrected following the model developed by Landauer to take into account the relative density of the samples.[33] Above room temperature, the thermal conductivity of the quaternary compounds decreases with temperature up to 1000 K. These measurements, together with the thermopower data, clearly show that these samples do not experience minority carrier effect. At 1000 K, the thermal conductivity values range between 2.8 and 8 $W\ m^{-1}\ K^{-1}$, the lowest value being achieved for the maximum Te concentration, i.e., in the $x=1.0$ compound.

To separate the electronic and lattice contributions to the total thermal conductivity, the former has been estimated using the Wiedemann–Franz law

$$\lambda_e = \frac{LT}{\rho}, \quad (5)$$

where L is the Lorenz number. Previous high temperature experiments performed on the $Mo_{3-x}Ru_xSb_7$ and $Mo_3Sb_{7-x}Te_x$ compounds have shown that taking the value of a fully degenerate electron gas ($L_0=2.44\times 10^{-8}$ $V^2\ K^{-2}$) would result in unrealistic electronic contributions higher

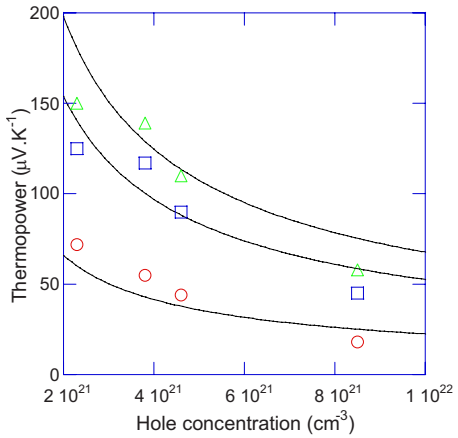

FIG. 3. (Color online) Hole concentration dependence of the thermopower measured at 300 (○), 700 (□), and 900 K (△). The solid lines stand for the best fit to the data according to the Eqs. (1)–(3).

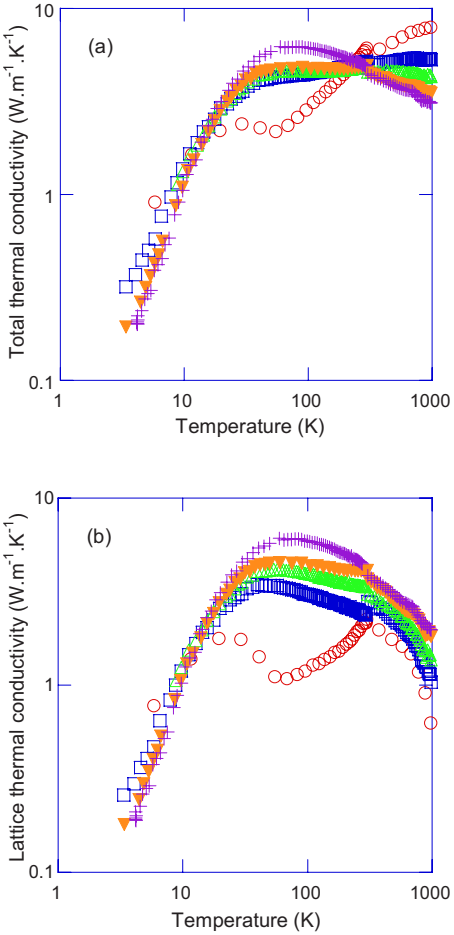

FIG. 4. (Color online) Temperature dependence of the total (a) and lattice (b) thermal conductivity of Mo_3Sb_7 (○) and of the $x=0.0$ (□), 0.25 (△), 0.50 (▼), and 1.0 (+) samples.

than the measured total thermal conductivity for low Ru and Te contents.[29,31] This clearly underlines that the degree of degeneracy together with acoustic phonon scattering must be taken into account to properly separate the two above-mentioned contributions. In this regard, the Lorenz number, with acoustic phonons as the main scattering source, can be more precisely estimated via the relation[32,7]

$$L = \left(\frac{k_B}{e}\right)^2 \left\{ \frac{3F_2(\eta)}{F_0(\eta)} - \left[\frac{2F_1(\eta)}{F_0(\eta)}\right]^2 \right\}. \quad (6)$$

Such determined values of L, reported in Table III at 300 and 900 K, substantially deviate from L_0. Consequently, as a first approximation, we used the values obtained at 900 K to separate the electronic and lattice contributions in the whole temperature range. It is worth mentionning that taking the exact value of L at each temperature to extract the lattice contribution at low temperature would not substantially modify the reported trends nor our analysis. The resulting temperature dependence of the lattice thermal conductivity is depicted in Fig. 4(b) for all samples studied. Above 300 K, the lattice thermal conductivity decreases with temperature to reach values ranging between 0.6 and 2.0 W m^{-1} K^{-1} at 1000 K. Though substituting on both sites increases the disorder in the crystal lattice, these values are similar to those measured in the ternary analogs.[29–31] Such a result is, however, not surprising given the similar molar masses and atomic radii of the Mo and Ru atoms on one hand and of the Sb and Te atoms on the other hand.

The variations in the lattice thermal conductivity values with x constitute one of the most intriguing and counterintuitive property of these materials. The increase in the disorder does not result in a decrease in the lattice thermal conductivity values but in its increase with the Te content in the whole temperature range. Such dependence mimics those reported in ternary alloys and might be explained by the exotic magnetic properties exhibited by Mo_3Sb_7.[12,14,26,27,29,31] In this material, the spin gap formation is associated to antiferromagnetically coupled molybdenum dimers.[14] The unusual thermal transport has been then tentatively ascribed to a strong phonons-dimers interaction.[12] Thorough investigations of the transport and magnetic properties of the ternary compounds have provided further evidence in favor of this picture since a partial substitution, irrespective of the crystallographic site, progressively suppresses the magnetic interactions and, concomitantly, the thermal conductivity recovers a conventional temperature dependence at low temperature.[26,27] Moreover, since mass fluctuation effects seem to be rather weak in the present case, similar lattice contributions may be expected. The Mo_3Sb_7 and $x=0.25$ compounds should be then characterized by lower Lorenz numbers than those estimated following Eq. (6). It would be therefore tempting to attribute this discrepancy to a breakdown of a single scattering mechanism and parabolic band model at low substitution levels as already highlighted in the $Mo_3Sb_{7-x}Te_x$ compounds.[31] On the other hand, the analysis of the transport data has shown the pertinence of this approach in the present case. This seeming contradiction may, therefore, suggest an alternative explanation. Rather than calling into question the validity of this model to estimate the electronic contribution, the lower lattice thermal conductivity displayed by the Mo_3Sb_7 compound may turn out to be an intrinsic property reflecting an additional efficient phonon scattering mechanism. The key and so far open question raised by this picture is, therefore, whether or not the magnetic interactions which are still present at low substitution levels are the central aspect explaining the observed behavior.

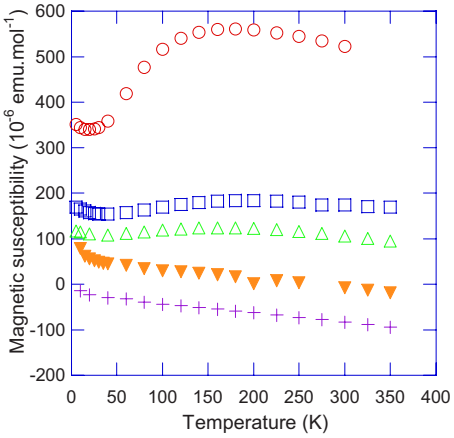

FIG. 5. (Color online) Temperature dependence of the magnetic susceptibility data of Mo_3Sb_7 (○) and of the $x=0.0$ (□), 0.25 (△), 0.50 (▼), and 1.0 (+) compounds.

The temperature dependence of the magnetic susceptibility, χ, illustrated in Fig. 5, seem indeed to support this scenario. For all samples, the χ values have been carefully extracted from the slope of the isothermal magnetization curves after subtraction of a small temperature-independent ferromagnetic contribution that saturates at low fields. The increase in the Te content markedly influences the magnetic properties of the Mo_3Sb_7 compound. The broad hump centered around 180 K associated to the magnetic fluctuations is severely damped in the $x=0.25$ sample while a further increase in the Te content completely suppresses this feature. Such variation upon alloying is consistent with the idea that the magnetic interactions associated to the molybdenum dimers in Mo_3Sb_7 are progressively suppressed as already shown in the Te and Ru ternary analogs.[26,27] This may constitute an experimental evidence of an intimate interplay between the magnetic interactions and the variations in the thermal conductivity in these materials. For the maximum Te content that can be achieved, the negative χ values observed in the whole temperature range are indicative of diamagnetic behavior. The decrease in the absolute χ values corroborates a rigid-band approximation in which electron filling induced by Ru and Te substitutions should lead to decreased densities of states at the Fermi level $N(E_F)$ and thus, to lower Pauli paramagnetic susceptibilities. The resulting behavior for high Te contents is then dominated by core diamagnetism.

Based on the measured transport properties, the dimensionless figure of merit ZT can be then calculated (Fig. 6). It must be mentioned that the electrical resistivity and Seebeck coefficient were extrapolated above 800 K and 900 K, respectively, assuming a linear temperature dependence up to 1000 K. This hypothesis is not only supported by the absence of minority carriers effect up to 1000 K as revealed by the

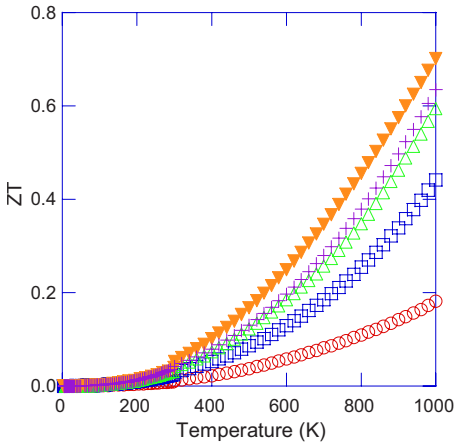

FIG. 6. (Color online) Temperature dependence of the dimensionless figure of merit *ZT* of Mo_3Sb_7 (○) and of the x=0.0 (□), 0.25 (△), 0.50 (▼), and 1.0 (+) samples.

thermal conductivity measurements but also by transport properties studies carried out on the ternary systems.[29–31] For all samples, the *ZT* values increase monotonically with temperature up to 1000 K. A maximum *ZT* value of 0.70 is achieved at 1000 K in the $Mo_{2.7}Ru_{0.3}Sb_6Te$ compound. This value is slightly higher than those obtained in the ternary counterparts and similar to the best *ZT* value of the state-of-the-art thermoelectric materials operating in the 900–1200 K temperature range.[29–31,34] Thus, among all, this result positions this material as an interesting candidate for power generation applications.

IV. CONCLUSION

Transport property measurements coupled with low temperature galvanomagnetic and magnetic properties experiments have been carried out from 2 up to 1000 K on polycrystalline $Mo_{2.5}Ru_{0.5}Sb_{7-x}Te_x$ samples. None of the studied samples displays semiconductinglike behavior revealing that this double substitution does not provide an alternative way to drive the system into a semiconducting state. The absence of a metal-insulator transition is most likely related to the solubility limit of Ru that prevents two electrons per formula unit to be added as revealed by XRPD and EPMA studies. The simultaneous increase in the electrical resistivity and the thermopower faithfully reflects the decrease in the hole concentration with the Te content as shown by Hall effect experiments. A single parabolic band model with acoustic phonon scattering provides a pertinent theoretical background to analyze the transport data of these materials. However, such a simple model might be inadequate to properly estimate the electronic thermal conductivity and thus, to reliably extract the lattice contribution at low substitution levels. Alternatively, this breakdown might constitute an evidence in favor of an additional and efficient scattering mechanism of phonons most likely associated with the antiferromagnetic dimers. Magnetic susceptibility data show that increasing the Te content results in a progressive disappearance of the magnetic interactions which might be at the core of the surprising increase in the total thermal conductivity with x. The beneficial influence of this double substitution on the thermoelectric properties is reflected by a maximum *ZT* value of ~0.70 at 1000 K achieved in the $Mo_{2.5}Ru_{0.5}Sb_{6.5}Te_{0.5}$ compound. This result shows that these materials are possible candidates for power generation applications. To further enhance the *ZT* values, there is still considerable phase space to be explored. It may be worthwhile to substitute Mo and/or Sb by other elements such as Fe or Os. Such substitutions may help to lower the thermal conductivity by increasing mass fluctuations and may lead to a metal-insulator transition paving the way to finely tune the power factor.

[1]S. M. Kauzlarich, S. R. Brown, and G. J. Snyder, Dalton Trans. 2099 (2007).
[2]F. Gascoin, S. Ottensmann, D. Stark, S. M. Haile, and G. J. Snyder, Adv. Funct. Mater. **15**, 1860 (2005).
[3]X.-J. Wang, M.-B. Tang, J.-T. Zhao, H.-H. Chen, and X.-X. Yang, Appl. Phys. Lett. **90**, 232107 (2007).
[4]C. Yu, T. J. Zhu, S. N. Zhang, X. B. Zhao, J. He, Z. Su, and T. M. Tritt, J. Appl. Phys. **104**, 013705 (2008).
[5]X.-J. Wang, M.-B. Tang, H.-H. Chen, X.-X. Yang, J.-T. Zhao, U. Burkhardt, and Yu. Grin, Appl. Phys. Lett. **94**, 092106 (2009).
[6]H. Zhang, J.-T. Zhao, Yu. Grin, X.-J. Wang, M.-B. Tang, Z.-Y. Man, H.-H. Chen, and X.-X. Yang, J. Chem. Phys. **129**, 164713 (2008).
[7]H. J. Goldsmid, *Thermoelectric Refrigeration* (Temple Press Books Ltd, London, 1964).
[8]S. R. Brown, S. M. Kauzlarich, F. Gascoin, and G. J. Snyder, Chem. Mater. **18**, 1873 (2006).
[9]S. R. Brown, E. S. Toberer, T. Ikeda, C. A. Cox, F. Gascoin, S. M. Kauzlarich, and G. J. Snyder, Chem. Mater. **20**, 3412 (2008).
[10]E. S. Toberer, C. A. Cox, S. R. Brown, T. Ikeda, A. F. May, S. M. Kauzlarich, and G. J. Snyder, Adv. Funct. Mater. **18**, 2795 (2008).
[11]E. S. Toberer, S. R. Brown, T. Ikeda, S. M. Kauzlarich, and G. J. Snyder, Appl. Phys. Lett. **93**, 062110 (2008).
[12]C. Candolfi, B. Lenoir, A. Dauscher, E. Guilmeau, J. Hejtmanek, J. Tobola, B. Wiendlocha, and S. Kaprzyk, Phys. Rev. B **79**, 035114 (2009).
[13]C. Candolfi, B. Lenoir, A. Dauscher, C. Bellouard, J. Hejtmanek, E. Santava, and J. Tobola, Phys. Rev. Lett. **99**, 037006 (2007).
[14]V. H. Tran, W. Miiller, and Z. Bukowski, Phys. Rev. Lett. **100**, 137004 (2008).
[15]Z. Bukowski, D. Badurski, J. Stepien-Damm, and R. Troc, Solid State Commun. **123**, 283 (2002).
[16]R. Khasanov, P. W. Klamut, A. Shengelaya, Z. Bukowski, I. M. Savic, C. Baines, and H. Keller, Phys. Rev. B **78**, 014502 (2008).
[17]V. H. Tran, A. D. Hillier, D. T. Adroja, and Z. Bukowski, Phys. Rev. B **78**, 172505 (2008).
[18]V. H. Tran, W. Miiller, and Z. Bukowski, Acta Mater. **56**, 5694 (2008).
[19]T. Koyama, H. Yamashita, Y. Takahashi, T. Kohara, I. Watanabe, Y. Tabata, and H. Nakamura, Phys. Rev. Lett. **101**, 126404 (2008).
[20]A. B. Karki, D. P. Young, P. W. Adams, E. K. Okudzeto, and Y. Julia Chan, Phys. Rev. B **77**, 212503 (2008).
[21]B. Wiendlocha, J. Tobola, M. Sternik, S. Kaprzyk, K. Parlinski, and A. M. Oles, Phys. Rev. B, **78**, 060507(R) (2008).
[22]C. Candolfi, B. Lenoir, A. Dauscher, J. Hejtmanek, E. Santava, and J. Tobola, Phys. Rev. B **77**, 092509 (2008).
[23]T. Koyama, H. Yamashita, T. Kohara, Y. Tabata, and H. Nakamura, Mater. Res. Bull. **44**, 1132 (2009).
[24]U. Häussermann, M. Elding-Ponten, C. Svensson, and S. Lidin, Chem.-Eur. J. **4**, 1007 (1998).
[25]E. Dashjav, A. Szczepenowska, and H. Kleinke, J. Mater. Chem. **12**, 345 (2002).
[26]C. Candolfi, B. Lenoir, A. Dauscher, J. Hejtmanek, B. Wiendlocha, and J. Tobola, Phys. Rev. B **79**, 235108 (2009).
[27]C. Candolfi, B. Lenoir, A. Dauscher, J. Hejtmanek, B. Wiendlocha, and J. Tobola, Phys. Rev. B **80**, 155127 (2009).
[28]C. Candolfi, B. Lenoir, J. Leszczynski, A. Dauscher, J. Tobola, S. J. Clarke, and R. I. Smith, Inorg. Chem. **48**, 5216 (2009).
[29]C. Candolfi, B. Lenoir, J. Leszczsynki, A. Dauscher, and E. Guilmeau, J. Appl. Phys. **105**, 083701 (2009).
[30]F. Gascoin, J. Rasmussen, and G. J. Snyder, J. Alloys Compd. **427**, 324

(2007).
[31]C. Candolfi, B. Lenoir, C. Chubilleau, A. Dauscher, and E. Guilmeau, J. Phys.: Condens. Matter **22**, 025801 (2010).
[32]V. I. Fistul, *Heavily Doped Semiconductors* (Plenum Press, New York, 1969).
[33]R. Landauer, J. Appl. Phys. **23**, 779 (1952).
[34]D. M. Rowe, *CRC Handbook of Thermoelectrics* (CRC Press, Boca Raton, FL, 1995).